

Direct Power Control of Three Phase PWM Rectifier based DSOGI-VF Estimator for No-Ideal Line Voltages Conditions

A. Rahab *, F.Senani **, H. Benalla***

* Laboratoire de l'Electrotechnique de Constantine (LEC), Faculté des Sciences de la Technologie, Université des frères Mentouri de Constantine 1, Ain el-bey 25000 Constantine, Algeria

** Laboratoire de l'Electrotechnique de Constantine (LEC), Faculté des Sciences de la Technologie, Université des frères Mentouri de Constantine 1, Ain el-bey 25000 Constantine, Algeria

*** Laboratoire de l'Electrotechnique de Constantine (LEC), Faculté des Sciences de la Technologie, Université des frères Mentouri de Constantine 1, Ain el-bey 25000 Constantine, Algeria

ABSTRACT

In this paper, direct power control (DPC) of three-phase pulse width-modulated rectifiers without line voltage sensors is presented. The new system is based on virtual flux (VF) using dual Second Order Generalized Integrator frequency located loop DSOGI-FLL estimator. In order to improve the VF-DPC performance of PWM rectifier, an improved observation method of virtual flux-linkage is proposed. To avoid the relevant problems of pure integrator, and to achieve the accurate observation of the grid voltage's phase, (SOGI-FLL) are used to displace the pure integrator. Theoretical principles of this method are discussed. This strategy is also investigated under unbalance and pre-distortion grid. A theoretical analysis of active and reactive power under a non-ideal source is clearly demonstrated. In order to calculate the compensated powers, the extraction of positive, negative, and harmonic sequences of voltage and current is needed and a multiple DSOGI-FLL method is used for rapid and accurate extraction. It is shown that the VFDP exhibits several advantages, particularly providing sinusoidal line current when the supply voltage is not ideal.

Keywords - Three-Phase Rectifier, DPC, Virtual Flux Estimation, DSOGI-FLL, no-ideal grid voltage

Date of Submission: 14-12-2017

Date of acceptance: 03-01-2018

I. INTRODUCTION

PWM AC/DC converters have several advantages such as low harmonic distortion of input currents, bi-directional power flow, high power factor and stable dc-link voltage [1]. Recently, due to the sharp increase of renewable energy sources connected to the grid, more and more converters are applied in wind turbines, photovoltaic system, fuel cells, energy storage system and flexible AC transmission system (FACTS) devices. At the same time, high power application in these renewable energy systems requires converters to operate more effectively in improving power quality and the transient stability [2]. Therefore, advanced control techniques are very necessary to fulfill these standards.

The three-phase pulse width-modulated rectifiers control approaches can be classified, as cited in the literature as a vector oriented control (VOC) and direct power control (DPC) [3], the vector control (VC) can be either based on grid voltage [4, 5, 6] or virtual flux (VF)[7] using proportional integral (PI) controllers. However, it has some disadvantages, such as its dependence on

the system parameters variation, that its performance largely depends on the tuning of the PI parameters [8]. In order to overcome complication due to the current control loops, an effective control, namely direct power control (DPC) has been developed [9]. Direct power control (DPC) strategy has become one of the hot research topics in recent Years, because of its fast dynamic response, simple structure, and high power factor, and so on [10, 11]. In general, the control of three-phase converter contains more sensors (DC voltage sensor, power grid voltage sensors and AC current sensors), which not only increases the volume of the system device, improves the system cost, but also reduces the system reliability [11].

The three-phase rectifier can be seen as a virtual AC motor, its virtual flux-linkage can be used to estimate the voltage of rectifier, But in the conventional virtual flux estimation of three-phase rectifier, there exists a pure integral link, and then the estimation process of virtual flux is inevitably affected by the initial value and the cumulative deviation of the integrator [11, 12 and 13, 14, 15, 16, 17]. The resolution of the problems of pure integration, more researchers focus on replacing the

pure integrator by using low-pass filters (LPFs), the initial value problem of pure integrator can be successfully solved[11],[15-17], however, the problem of amplitude and phase deviation is caused. In order to overcome the influence of integral initial value and cumulative deviation of pure integrator, and avoid the amplitude and phase deviation caused by first-order low-pass filter, several authors propose methods of estimation of the Virtual Flux such as [12], [18], based in pure integrator in conventional observer of virtual flux-linkage. In summary, the key to a successful operation of the DPC utilizing grid virtual flux estimation is dependent on the effectiveness of the virtual flux estimation procedure and the selection of the converter switching states [19].

This research proposes a new method for Virtual Flux estimation that is inherently capable of handling these problems; as a result a stable and smooth virtual flux estimated and sector detection with high precision. The suggested method is based on utilizing the Second Order Generalized Integrator (SOGI) reported in [14-16], and improved switching table defined in [20].

This paper is organized as follows: In Section 2, mathematical Model of three-phase PWM converter. In section 3 presents the VFDPD using Second Order Generalized Integrator frequency located loop (SOGI-FLL) system configuration and gives basic relations of virtual flux and powers estimators and proposed modified virtual flux direct power control MVFDPC when we have under unbalanced distorted grid voltage, Section 4 presented simulation results and discussion finally, the conclusion are provided in section 5

II. MODEL OF THREE-PHASE PWM CONVERTER

As we can see in figure 1, Block diagram for three-phase PWM rectifier. It is controlled using a VFDPD based SOGI flux estimation.

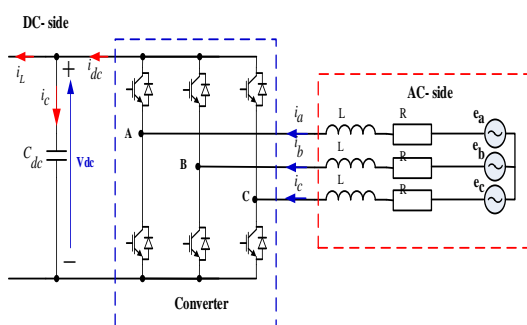


Fig. 1: Block diagram for three-phase PWM rectifier

The rectifier can be expressed, in a-b-c reference frame with following equations [10]:

$$\begin{bmatrix} e_a \\ e_b \\ e_c \end{bmatrix} = R \begin{bmatrix} i_a \\ i_b \\ i_c \end{bmatrix} + L \frac{d}{dt} \begin{bmatrix} i_a \\ i_b \\ i_c \end{bmatrix} + \begin{bmatrix} V_A \\ V_B \\ V_C \end{bmatrix} \quad (1)$$

Where: L and R are the inductance and resistance of the chokes, respectively e_a, e_b, e_c, i_a, i_b and i_c are the electrical grid voltage and current, V_A, V_B, V_C are the AC side voltages of the rectifier.

The AC rectifier's voltages V_A, V_B and V_C are defined as:

$$\begin{cases} V_A = \frac{V_{dc}}{3} (2S_a - S_b - S_c) \\ V_B = \frac{V_{dc}}{3} (-S_a + 2S_b - S_c) \\ V_C = \frac{V_{dc}}{3} (-S_a - S_b + 2S_c) \end{cases} \quad (2)$$

S_a, S_b and S_c are the switching states of the rectifier show figure1.

The relationship between the AC side rectifier currents i_a, i_b and i_c and the DC bus voltage V_{dc} can be written as:

$$C_{dc} \frac{dV_{dc}}{dt} = S_a i_a + S_b i_b + S_c i_c - i_L \quad (3)$$

Where C_{dc} is the dc link capacitance, i_L the load current

III. CONTROL OF THE THREE-PHASE PWM RECTIFIER BASED (DSOGI-FLL)

III.1 Virtual Flux based Direct Power Control (VFDPD)

The virtual flux (VF) concept which relates the grid voltage and the ac-side inductors to a virtual ac motor hence; R and L represent the stator resistance and the stator leakage resistance of the virtual motor. The line-to-line grid voltages e_{ab}, e_{bc}, e_{ca} would be induced by a virtual air gap flux. In other perspective, the integration of the line voltages leads to a virtual line vector Ψ_L . Figure 2 shows the basic scheme of VF-DPC.

The command active power (P_{ref}) and reactive power (Q_{ref}) are compared with the estimated P and Q values via active and reactive power hysteresis controllers, respectively. The digitized output signals (S_P) and (S_Q) and the VF vector position ($\theta_{\Psi L}$) are used to select the appropriate voltage vector according to the switching table defined in [20]. The advantage of choosing this improved table because it gives the best results, reducing the total harmonic distortion (THD) of line currents and switching losses [20].

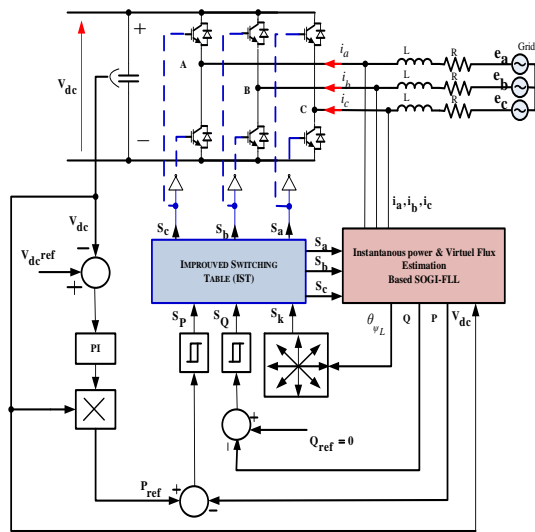


Fig. 2 Virtual-flux based direct power control (VF-DPC) scheme.

III.1.1 Power Estimation Based on Virtual Flux

The virtual flux components are calculated in stationary (α - β) coordinates system as [11]

$$\psi_{La} = \int \left(u_{conca} + L \frac{di_{La}}{dt} \right) dt \quad (4)$$

$$\psi_{L\beta} = \int \left(u_{cony\beta} + L \frac{di_{L\beta}}{dt} \right) dt \quad (5)$$

Then, equations (6) and (7) are used to estimate the active and reactive power [10].

$$P = \omega (\psi_{La} i_{L\beta} - \psi_{L\beta} i_{La}) \quad (6)$$

$$Q = \omega (\psi_{La} i_{La} + \psi_{L\beta} i_{L\beta}) \quad (7)$$

The VF vector position $\theta_{\psi_L} = \tan^{-1} \left(\frac{\psi_{La}}{\psi_{L\beta}} \right)$ is used in

VF-DPC scheme to select the appropriate converters voltage vector according to the improved switching table defined in [20].

III.1.2 SOGI-FLL Flux Estimation

a. Structure of SOGI

The structure of the SOGI is shown on fig. 3(a) the first output (u') of the SOGI is in phase and with the same amplitude with the input (u), the second output (qu') is shifted of 90° with the same amplitude, (the letter 'q' is for indicating that this output is in quadrature with (u')). The two output can then be used for computing magnitude and phase of input (u). K is the damping Factor of the filter, a gain of great value gives a quick response but can affect the accuracy of the filter and a gain of low value can cause a very long transient response. Then, taking into account all these circumstances the value optimal of gain K is $(\sqrt{2})$ [14, 15].

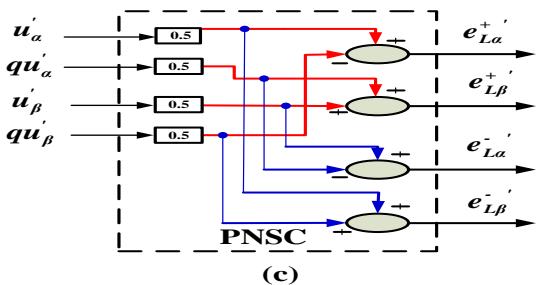
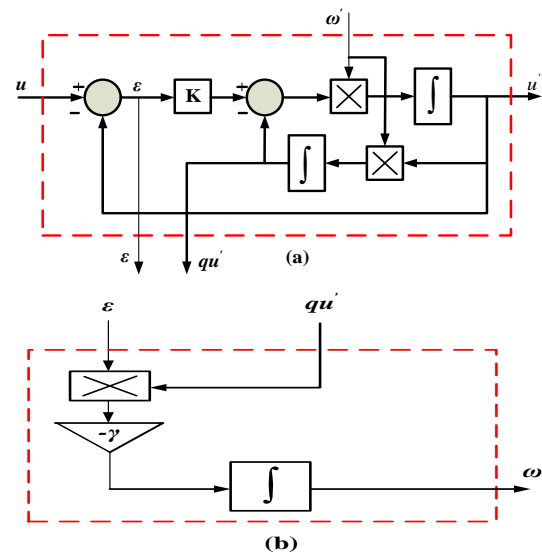


Fig. 3 Block diagrams (a) SOGI-QSG scheme, (b) FLL Block. (c) PNSC detection

The transfer functions represented by (8), (9) and (10) for band pass filter (BPF) and low-pass filter (LPF), passes bandfilter with a null (gain) at the frequency (ω') respectively.

$$D(S) = \frac{u'}{u}(S) = \frac{k\omega' S}{S^2 + k\omega' S + \omega'^2} \quad (8)$$

$$Q(S) = \frac{qu'}{u}(S) = \frac{k\omega'^2}{S^2 + k\omega' S + \omega'^2} \quad (9)$$

$$E(S) = \frac{\epsilon}{u}(S) = \frac{S^2 + \omega'^2}{S^2 + k\omega' S + \omega'^2} \quad (10)$$

b. Frequency Locked Loop (FLL)

The Frequency-Locked Loop (FLL) structure, shown in Fig. 3(b) can be used to measure the angular frequency ω of the input signal v (in this case, ω' is the output or estimated angular frequency of the input signal v) without using trigonometric functions and making easier its implementation in conventional microcontrollers [21,22].

The introduction of the FLL allows to adapt the input frequency of the SOGI with the frequency of the signal is filtered. The SOGI account as a good

solution for the estimation of the Virtual flux under a disturbed network.

As already seen previously, the second output of the SOGI is a signal of the same amplitude to that of the input but shift of 90^0 , So we can use the SOGI to integrate (4),(5) and by consequence estimate the virtual flux [14].

Under a balanced network, the virtual flux can be estimated by the SOGI as illustrated in fig.4.

Where: **RVC**: resistance voltage compensation
IFC: inductance flux compensation

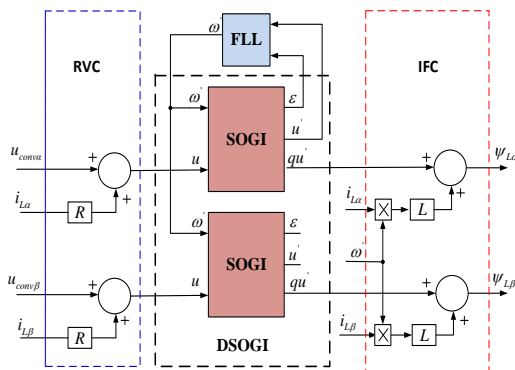


Fig. 4 Virtual flux estimator under balanced grid voltage using SOGI-FLL.

When the grid is unbalanced, the virtual flux can be estimated by the SOGI as illustrated in Fig. 5.

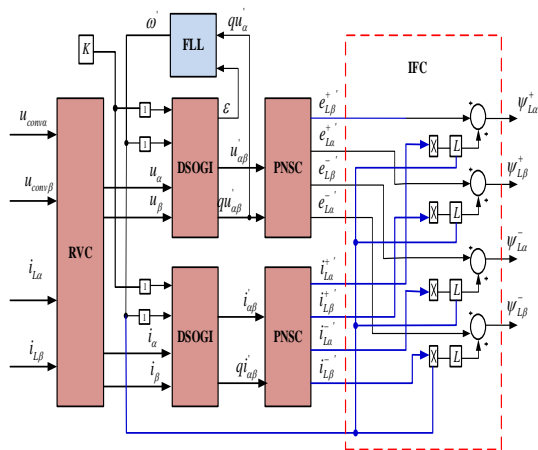


Fig.5 Virtual flux estimator under unbalanced grid using DSOGI-FLL.

In the general case, unbalanced source and contains harmonics, the VF can be estimated by multiple second order generalized integrators (MSOGI) which are frequency-adaptive by using a frequency-locked loop (FLL) as illustrated in Fig. 6, [22].

The positive and negative sequence component

(PNSC) $(V_{\alpha\beta p}^+, V_{\alpha\beta p}^-)$ is given by (11), (12),

Where $q = e^{-j\frac{\pi}{2}}$ is a phase-shift operator to obtain the in-quadature version of an original waveform (90-degrees lag) [22].

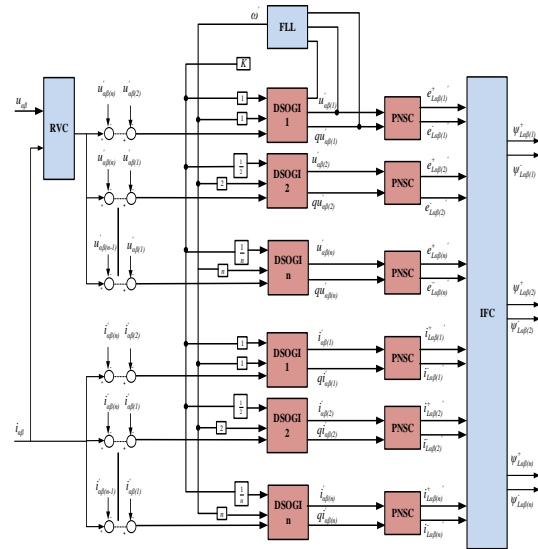


Fig. 6 Virtual flux estimator under unbalance and pre-distorted supply voltage based (MSOGI).

$$\begin{bmatrix} V_{\alpha}^+ \\ V_{\beta}^+ \end{bmatrix} = \frac{1}{2} \begin{bmatrix} 1 & -q \\ q & 1 \end{bmatrix} \begin{bmatrix} V_{\alpha}' \\ V_{\beta}' \end{bmatrix} \quad (11)$$

$$\begin{bmatrix} V_{\alpha}^+ \\ V_{\beta}^+ \end{bmatrix} = \frac{1}{2} \begin{bmatrix} 1 & q \\ -q & 1 \end{bmatrix} \begin{bmatrix} V_{\alpha}' \\ V_{\beta}' \end{bmatrix} \quad (12)$$

III.2 Modified virtual flux direct power control MVDPC

Based for the topological structure of three-phase voltage-type PWM rectifier is shown in Figure 1, when the grid voltage is unbalanced, according to symmetric decomposition theory, an unbalanced three-phase system can be discomposed in three balanced symmetric three phase system, the zero sequence, the positive sequence, and the negative sequence, which can be expressed as[23]:

$$\begin{bmatrix} x^0 \\ x^+ \\ x^- \end{bmatrix} = \frac{1}{3} \begin{bmatrix} 1 & 1 & 1 \\ 1 & a & a^2 \\ 1 & a^2 & a \end{bmatrix} \begin{bmatrix} x_a \\ x_b \\ x_c \end{bmatrix} \quad (13)$$

Where subscript (0) and (+), (-) denote zero sequence, the positive sequence, and the negative sequence,

and $a = e^{j(\frac{2\pi}{3})}$, the sum of the currents will always be zero (in this analysis assume a three-wire connection system), as a result, the zero of the currents will be zero. In this work, unbalance and fifth order harmonic components in the supply voltage are taken into account. In stationary reference frames, when the supply voltage

unbalanced and distorted, the voltage and current of grid are expressed in (14), (15)

$$E_{\alpha\beta} = e_{\alpha} + j e_{\beta} = (e_{\alpha}^{+} + e_{\alpha}^{-} + e_{\alpha}^5) + j(e_{\beta}^{+} + e_{\beta}^{-} + e_{\beta}^5) \quad (14)$$

$$I_{\alpha\beta} = i_{\alpha} + j i_{\beta} = (i_{\alpha}^{+} + i_{\alpha}^{-} + i_{\alpha}^5) + j(i_{\beta}^{+} + i_{\beta}^{-} + i_{\beta}^5) \quad (15)$$

$$\psi_{\alpha\beta} = \psi_{\alpha} + j \psi_{\beta} = \left(\begin{array}{l} (\psi_{\alpha}^{+} + \psi_{\alpha}^{-} + \psi_{\alpha}^5) + \\ j(\psi_{\beta}^{+} + \psi_{\beta}^{-} + \psi_{\beta}^5) \end{array} \right) \quad (16)$$

After substituting the flux and current by their values shown in (15) and (16), the active and reactive powers results can be regrouped in four terms:

$$P = \frac{3}{2}(P_0 + P_1 + P_2 + P_3) \quad (17)$$

$$Q = \frac{3}{2}(Q_0 + Q_1 + Q_2 + Q_3) \quad (18)$$

Where:

$$P_0 = \omega \left(\begin{array}{l} \psi_{L\alpha}^{+} i_{L\beta}^{+} - \psi_{L\beta}^{+} i_{L\alpha}^{+} + \psi_{L\alpha}^{-} i_{L\beta}^{-} - \psi_{L\beta}^{-} i_{L\alpha}^{-} + \\ \psi_{L\alpha}^5 i_{L\beta}^5 - \psi_{L\beta}^5 i_{L\alpha}^5 \end{array} \right) \quad (19)$$

$$P_1 = \omega (\psi_{L\alpha}^{+} i_{L\beta}^{-} - \psi_{L\beta}^{+} i_{L\alpha}^{-} + \psi_{L\alpha}^{-} i_{L\beta}^{+} - \psi_{L\beta}^{-} i_{L\alpha}^{+}) \quad (20)$$

$$P_2 = \omega (\psi_{L\alpha}^{+} i_{L\beta}^5 - \psi_{L\beta}^{+} i_{L\alpha}^5 + \psi_{L\alpha}^5 i_{L\beta}^{+} - \psi_{L\beta}^5 i_{L\alpha}^{+}) \quad (21)$$

$$P_3 = \omega (\psi_{L\alpha}^5 i_{L\beta}^{-} - \psi_{L\beta}^5 i_{L\alpha}^{-} + \psi_{L\alpha}^{-} i_{L\beta}^5 - \psi_{L\beta}^{-} i_{L\alpha}^5) \quad (22)$$

$$Q_0 = \omega \left(\begin{array}{l} \psi_{L\alpha}^{+} i_{L\alpha}^{+} + \psi_{L\beta}^{+} i_{L\beta}^{+} + \psi_{L\alpha}^{-} i_{L\alpha}^{-} + \psi_{L\beta}^{-} i_{L\beta}^{-} + \\ \psi_{L\alpha}^5 i_{L\alpha}^5 + \psi_{L\beta}^5 i_{L\beta}^5 \end{array} \right) \quad (23)$$

$$Q_1 = \omega (\psi_{L\alpha}^{+} i_{L\alpha}^{-} + \psi_{L\beta}^{+} i_{L\beta}^{-} + \psi_{L\alpha}^{-} i_{L\alpha}^{+} + \psi_{L\beta}^{-} i_{L\beta}^{+}) \quad (24)$$

$$Q_2 = \omega (\psi_{L\alpha}^{+} i_{L\alpha}^5 + \psi_{L\beta}^{+} i_{L\beta}^5 + \psi_{L\alpha}^5 i_{L\alpha}^{+} + \psi_{L\beta}^5 i_{L\beta}^{+}) \quad (25)$$

$$Q_3 = \omega (\psi_{L\alpha}^5 i_{L\alpha}^{-} + \psi_{L\beta}^5 i_{L\beta}^{-} + \psi_{L\alpha}^{-} i_{L\alpha}^5 + \psi_{L\beta}^{-} i_{L\beta}^5) \quad (26)$$

P_0, Q_0 : are the average active and reactive powers delivered to DC-link voltage and it is a constant power.

P_1, Q_1 : represents the interaction between the positive and negative sequence of fluxes and currents that generates an oscillation in the active and reactive power with a frequency that is twice the fundamental frequency.

P_2, Q_2 : represents the interaction between the positive and the fifth harmonic sequences of the fluxes and currents that generates an oscillation in the active power with a frequency that is 4 times the fundamental frequency.

P_3, Q_3 : represents the interaction between the negative and fifth harmonic sequences of the fluxes and current that generates an oscillation in the active power with a frequency that is 6 times the fundamental frequency.

There are many control laws that can be applied in the proposed control, to obtain sinusoidal and

balanced line currents, the negative sequence component's and 5th harmonic sequence must be eliminated. Notice that $i_{L\alpha}^{-}, i_{L\beta}^{-}, i_{L\alpha}^5$ and $i_{L\beta}^5$ only operate in P_1 and Q_1 , therefore, in order to $i_{L\alpha}^{-} = i_{L\beta}^{-} = i_{L\alpha}^5 = i_{L\beta}^5 = 0$, in P_3 , and Q_3 should be kept zeros, and at the (14) and (15) can be written as (17) and (18).

$$P = \frac{3}{2} \omega \left(\begin{array}{l} \psi_{L\alpha}^{+} i_{L\beta}^{+} - \psi_{L\beta}^{+} i_{L\alpha}^{+} + \psi_{L\alpha}^{-} i_{L\beta}^{-} - \psi_{L\beta}^{-} i_{L\alpha}^{-} \\ + \psi_{L\alpha}^5 i_{L\beta}^5 - \psi_{L\beta}^5 i_{L\alpha}^5 \end{array} \right) \quad (27)$$

$$Q = \frac{3}{2} \omega \left(\begin{array}{l} \psi_{L\alpha}^{+} i_{L\alpha}^{+} + \psi_{L\beta}^{+} i_{L\beta}^{+} + \psi_{L\alpha}^{-} i_{L\alpha}^{-} + \psi_{L\beta}^{-} i_{L\beta}^{-} \\ + \psi_{L\alpha}^5 i_{L\alpha}^5 + \psi_{L\beta}^5 i_{L\beta}^5 \end{array} \right) \quad (28)$$

Under the balanced and perfectly sinusoidal grid voltage supply, there only exists a positive sequence component, and the powers can be described as:

$$P = \frac{3}{2} \omega (\psi_{L\alpha}^{+} i_{L\beta}^{+} - \psi_{L\beta}^{+} i_{L\alpha}^{+}) \quad (29)$$

$$Q = \frac{3}{2} \omega (\psi_{L\alpha}^{+} i_{L\alpha}^{+} + \psi_{L\beta}^{+} i_{L\beta}^{+}) \quad (30)$$

It can be seen from equations (27) and (28) that we want to eliminate the effect of the negative component and fifth order harmonic components of the grid; the active and reactive power compensated components can be obtained as:

$$P_{comp} = -\frac{3}{2} \omega (\psi_{L\alpha}^{-} i_{L\beta}^{+} - \psi_{L\beta}^{-} i_{L\alpha}^{+} + \psi_{L\alpha}^5 i_{L\beta}^{+} - \psi_{L\beta}^5 i_{L\alpha}^{+}) \quad (31)$$

$$Q_{comp} = -\frac{3}{2} \omega (\psi_{L\alpha}^{-} i_{L\beta}^{+} + \psi_{L\beta}^{-} i_{L\beta}^{+} + \psi_{L\alpha}^5 i_{L\alpha}^{+} + \psi_{L\beta}^5 i_{L\beta}^{+}) \quad (32)$$

The modified DPC strategy based on the idea of injecting the active and reactive power compensated components in the original referenced power to achieve control objectives. Fig.7 shows the control diagram.

The new power references that can achieve sinusoidal and symmetric stator current as:

$$P_{ref} = P_{const} + P_{comp} \quad (33)$$

$$Q_{ref} = Q_{const} + Q_{comp} \quad (34)$$

Where P_{const} and Q_{const} are the original constant power reference under normal grid conditions.

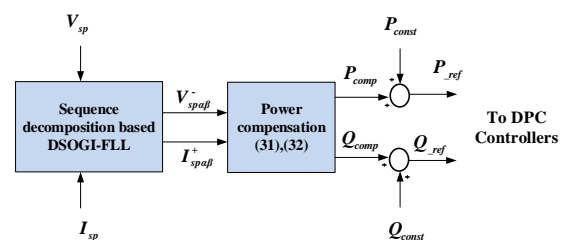


Fig. 7 Control strategy under unbalance and pre-distorted supply voltage

IV. SIMULATION RESULTS

For the validation of the proposed DPC strategy, the system has been modelled and built in MATLAB/SIMULINK software environment and tested under various conditions.

The converter dc link voltage is set at 180 V. The control of three phase rectifier aims to maintain a constant dc-link voltage, and it is controlled using VFDP method based SOGI-FLL virtual flux estimator. Starting procedure is not relevant to this paper and not shown in the results. The main electrical parameters of the system are given in table1.

Table 1. Parametresof the power circuit[24]

Line resistance	R=0.56Ω
Line inductance	L=19.5mH
DC-link capacitor	Cdc=1100μF
Load resistance	R _L =68.6Ω
Line to line ac voltage	e _{ab} =180V rms
Line frequency	f=50Hz
DC-link voltage	V _{dc} =180V

Parameters of DSOGI-FLL

- $\Gamma = 100$ (gain to the settling time of the FLL block)
- $k = \sqrt{2}$ (gain of the SOGI)

The system is analysed during steady state and transients conditions at three case presented in table2

Table 2. Case Simulation Study OF VFDP and M-VFDP

CASE	POWER SUPLY	Duration (s)	appeliez technique
1	Balanced	0 to 1 s	VFDP
	Unbalanced (15% supply voltages)	1 s to 1.1 s	VFDP
	Unbalanced (15% supply voltages)	1.1 s to 1.2s	M-VFDP
2	Balanced	0 to 1 s	VFDP
	Distorsed(20 % of 5 th harmonic)	1 s to 1.1s	VF-DPC
	Distorsed (20 % of 5 th harmonic)	1.1 s to 1.2s	M-VFDP
3	Balanced	0 to 1 s	VFDP
	Unbalanced distorsed (15% supply voltages) and (20 % of 5 th harmonic)	1s to 1.1 s	VFDP
	Unbalanced distorsed (15% supply voltages) and (20 % of 5 th harmonic)	1.1 s to 1.2	M-VFDP

IV.1 Simulation result of case 1:

Under balanced line voltage conditions. The control strategy of the VFDP-based SOGI estimator provides balanced and sinusoidal grid currents see fig. 8 at (t=0 s to t= 1s). At (t= 1s to 1.15 s) the shape of the line current is unbalanced and contains the harmonic of the 3rd order, see fig. 8 (c) and fig. 9 (b), the latter caused by the presence of an unbalanced network voltage.as well at (t=0s to t= 1s), the VFDP introduced very good performance under ideal unbalanced voltage.

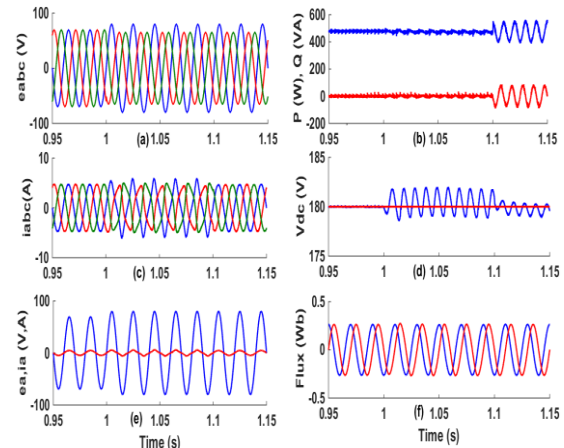


Fig.8 Simulation results from case1 (a) three phase voltage supply (b) active power in red reactive power in blue. (c) Grid currents. (d) DC link voltage in blue, reference DC voltage in red. (e) 1st phase voltage and current. (f) Estimated virtual flux ($\psi_{L\alpha}^+$ and $\psi_{L\beta}^+$)

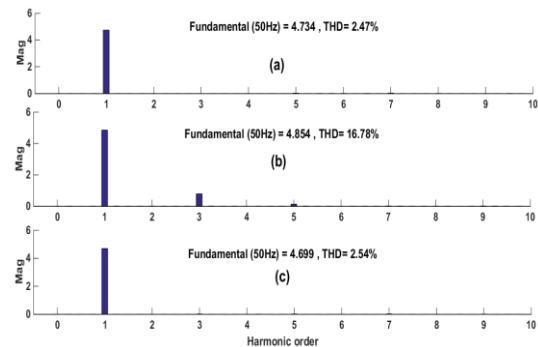


Fig. 9 Spectra of grid currents in case1. (a) Under unbalanced grid voltage condition using VFDP. (b) Under unbalanced grid voltage condition using VFDP. (c) Under unbalanced grid voltage condition using MVFDP.

At (t=1.1s) It can be seen that the active and reactive power oscillate at twice the grid frequency around their rated values. While the power ripples, resulting from an unbalanced part of the supply voltage that it still exists. On the other hand, at (t=0 to t 1s) from fig.8 (d) it can be seen that the PI controller could successfully maintain a fixed DC voltage value (180 V). The presence of an unbalance

in voltage supply creates pulsation terms in output DC-link voltage the frequency of the resulting oscillations is twice the input frequency show Fig. 8 (d).

After applying the MVFDPC compensation control strategy the low order harmonics of the line currents were eliminated and balanced currents were generated, and the unit power factor was obtained in unbalanced network voltage conditions. Fig. 8 (c, e) at (1.1 s to 1.15 s).

The frequency spectra in this case clearly show that the low-order harmonics can be reduced by employing the modified control strategy (MVFDPC) under unbalanced voltage supply. The total harmonic distortion (THD) of Input currents under ideal supply is 2.47% and it is increased to 16.78% under unbalanced supply, and after applying the MVFDPC strategy the THD is decreased to 2.54%, which meets the IEEE standard 519-1992.

IV.2 Simulation result case 2:

The presence of the 5th harmonic in the voltage supply figure creates reduced pulsation content at (6w) frequency for DC-link voltage output as shown in fig. 10 (d). Fig. 10 (b) summarizes the behavior of the system using (VFDPC and MVFDPC) control strategy in terms of input power under different supply voltage conditions. At (t= 0 to 1.2 s) , (VFDPC an MVFDPC) control strategy introduced very good performance under balanced or distorted voltage condition where the active power is set to their rated value without oscillation envisaged and at the same time the reactive power is maintained at zero Q = 0 VAR. without oscillation envisaged.

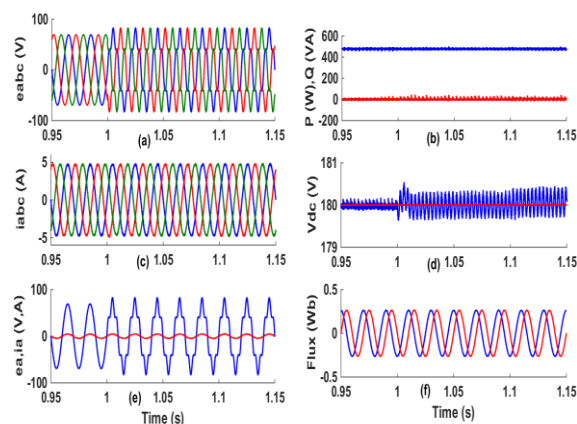


Fig. 10 Simulation results from case2 (a) three phase voltage supply (b) active power in red reactive power in blue. (c) Grid currents. (d) DC link voltage in blue, reference DC voltage in red. (e) 1st phase voltage and current. (f) Estimated virtual flux ($\Psi_{L\alpha}^+$ and $\Psi_{L\beta}^+$)

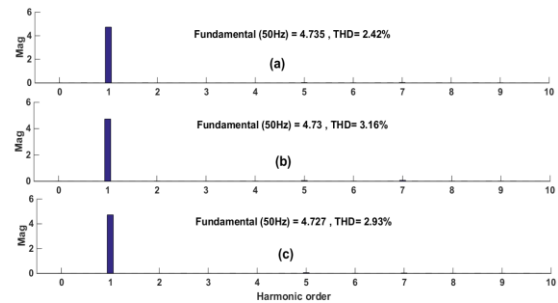


Fig. 11 Spectra of grid currents in case2. (a) Under unbalanced grid voltage condition using VFDPC. (b) Under unbalanced grid voltage condition using VFDPC. (c) Under unbalanced grid voltage condition using MVFDPC

The THD of input currents for the MVFDPC control strategy is only 2.93% and it is 3.16 % for the VFDPC control strategy with improved switching table under distorted power supply show fig. 11 (b-c).

The VFDPC scheme with improved switching table [20] is able to produce almost sinusoidal phase currents with unity power factor as shown In Fig. 10(c) and fig. 10(e) respectively.

IV.3 Simulation results case 3

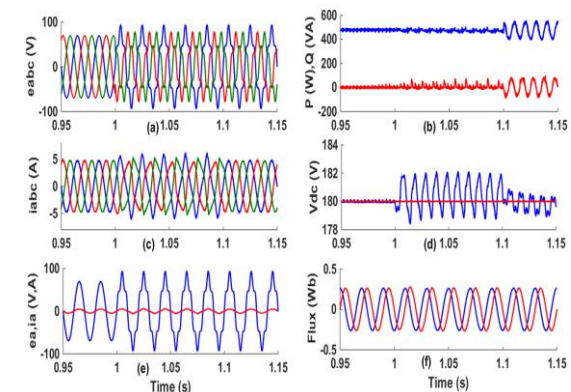


Fig.12 Simulation results from case3 (a) three phase voltage supply (b) active power in red reactive power in blue. (c) Grid currents. (d) DC link voltage in blue, reference DC voltage in red. (e) 1st phase voltage and current. (f) Estimated virtual flux ($\Psi_{L\alpha}^+$ and $\Psi_{L\beta}^+$)

Fig. 12(a) shows the behavior of the 2-level PWM converter controlled by the proposed strategy under totally unbalanced distorted voltage supply. At (t=0 to t= 1 s) the line currents are very sinusoidal fig. 12 (c) and the total harmonic distortion (THD) is only 2.42% fig. 13(a), due to the excellent control ability of the VFDPC control method. However, the line currents are seriously distorted when the grid voltage is unbalanced and distorted at (t=1 s to t= 1.1 s), the THD is 16.81 % with prominent (3th, 5th,

7th, 9th ...) order harmonic component, as shown in

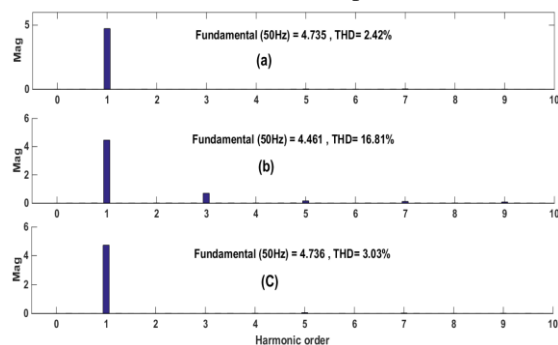


Fig. 13 Spectra of grid currents in case3. (a) Under balanced grid voltage condition using VFDP. (b) Under unbalanced grid voltage condition using VFDP. (c) Under unbalanced grid voltage condition using MVFDPC

After integrating the power compensation schemes into the VFDP method, the THD of the line current is reduced considerably to only 3.03%, as shown in Fig. 13(c). This demonstrates the effectiveness of the proposed MVFDPC scheme for power quality improvement. As shown in Fig. 12 (b) at (1=0 s to t=1.1s), all waveforms of active and reactive power are constant at (1=0 s to t=1.1s), no significant ripples. However, after integrating MVFDPC compensation method, there are many oscillations in active and reactive power. Active and reactive power oscillates at twice the grid frequency. The presence of both an unbalance and a 5th harmonic in the voltage supply creates pulsation terms in the output DC-link voltage shown in Fig. 12 (d). In the three cases simulated, the DSOGI-FLL has a good behavior for estimated positive sequence components of virtual flux when unbalanced and distorted voltages in the 3-phase supply voltages are shown in Fig. 8 (f), Fig. 10 (f) and Fig. 12 (f).

V. CONCLUSION

This paper has proposed a modified VFDP strategy for a 3-phase 2-level rectifier supplied by a disturbed voltage source. In order to obtain balanced and sinusoidal grid currents under inappropriate voltage conditions, compensated powers are calculated and added to the original reference power to achieve balanced and high quality input current.

The phase, positive, negative, and harmonic sequences of the voltage and the current are extracted using the M SOGI-FLL. The proposed strategy is verified by simulation for three cases, which are unbalanced voltage, distorted voltage, and simultaneously unbalanced and distorted voltage. It proves its capability of yielding sinusoidal and balanced grid current with unity power factor under a severe non-ideal source. VFDP approach in combination with a DSOGI estimator and improved

Fig. 13(b).

switching table can address perfectly balanced/distorted grid voltage condition; meanwhile it suffers and gives unsatisfied performance during unbalanced power supply condition. In order to overcome this disadvantage, we have proposed an MVFDPC approach with compensated powers obtaining a very good power quality on the grid side with a satisfactory power factor and a low THD factor for the input current within the standard limits whatever the power grid.

REFERENCE

- [1] Hu J, Zhu J, Dorrell D.G. A comparative study of direct power control of AC/DC converters for renewable energy generation. in Proc. IEEE IECON 2011 - 37th Annual Conference on IEEE Industrial Electronics Society. 2011:3578- 3583.
- [2] Hu J, Zhu J, Dorrell D. G. Control strategies of variable-speed wind system under new grid code requirement—A survey. in Proc. IEEE 2010 36th Annual Conf. IECON '10. 2010 :3061-3066.
- [3] Allagui M, Hasnaoui O. A 2 MW direct drive wind turbine vector control and direct torque control techniques comparison. *J. energy South. Afr.* 2014; 25(2): 117-126.
- [4] Prasad A, Ziogas P, Manias S. An active power factor correction technique for three-phase diode rectifiers. *IEEE Trans. Power Electron.* 1991 ;6(1) :83–92.
- [5] Nor Azizah Yusoff, Azziddin M. Razali, Kasrul Abdul Karim, Tole Sutikno, Auzani Jidin. A Concept of Virtual-Flux Direct Power Control of Three-Phase AC-DC Converter. *International Journal of Power Electronics and Drive System (IJPEDS)*. 2017; 8(4): 1776- 1784.
- [6] Pedro V, Marques G. D. DC voltage control and stability analysis of PWM-voltage-type reversible rectifier. *IEEE Trans. Ind. Electron.* 1998 ;45(2) :263–273.
- [7] Li Xiang, Han Minxiao. Direct Virtual Power Control. *TELKOMNIKA Indonesian Journal of Electrical Engineering*. 2014; 12(7): 5144-5153.
- [8] Mohseni M, Islam S, Masoum M. A. S. Enhanced hysteresis-based current regulators in vector control of DFIG wind turbines. *IEEE Trans. Power Electron.* 2011 ;26(1) :223–234.
- [9] Noguchi T, Tomiki H, Kondo S, Takahashi I. Direct power control of PWM converter without power-source voltage sensors. *IEEE Transactions on Industry Applications*. 1998 ;34(3) : 473– 479.
- [10] Malinowski M, Kazmierkowski M. Simple Direct Power Control of Three-Phase PWM

- Rectifier Using Space Vector Modulation 'A Comparative Study'. *EPE Journal*. 2015 : 27-34.
- [11] Malinowski M, Kazmierkowski M.P, Hansen S, Blaabjerg F, Marques GD. Virtual-flux based Direct Power Control of Three-phase PWM Rectifiers. *IEEE Transactions on Industry Applications*. 2001 ; 37(4):1019-1027.
- [12] Bu W, Xu L. Direct Power Control Strategy of PWM rectifier Based on Improved Virtual Flux-Linkage observer. *Journal of Control Science and Engineering*. volume 2017.
- [13] Ketzer M B, Jacobina C B. Sensorless Control Technique for PWM Rectifiers With Voltage Disturbance Rejection and Adaptive Power Factor[J]. *IEEE Transactions on Industrial Electronics*. 2015; 62(2):1140-1151.
- [14] WU F J, Wang Z W, Sun L. Improved virtual flux-oriented vector control of PWM rectifier. *Journal Electric Machines and control*. 2008; 5 : 504-508.
- [15] Suul J A, Luna A, Rodriguez P, Undeland T. Virtual-Flux-Based Voltage-Sensor-Less PowerControl for Unbalanced Grid Conditions. *IEEE Transactions On Power Electronics*. 2012 ; 27(9).
- [16] Zhao R, Xin Z, Loh P C, Blaabjerg F. A Novel Flux Estimator Based on SOGI with FLL for Induction Machine Drives. Applied Power Electronics Conference and Exposition (APEC). 2016.
- [17] Zhao R, Xin Z, Loh P C, Blaabjerg F. A Novel Flux Estimator Based on Multiple Second- Order Generalized Integrators and Frequency-Locked Loop for Induction Motor Drives. *IEEE Transactions on Power Electronics*. 2017 ;32(8).
- [18] BU W , Xu L. Improved Virtual-Flux-Linkage Observation method of PWM Rectifier. *Applied Mechanics and Materials*. 2014 ; 678 :528-532.
- [19] Azziddin M. Razali, M. A. Rahman, Glyn George, Nasrudin A. Rahim. 'Analysis and Design of New Switching Lookup Table for Virtual Flux Direct Power Control of Grid-Connected Three-Phase PWMAC-DC Converter'. *IEEE TRANSACTIONS ON INDUSTRY APPLICATIONS* Vol. 51, No. 2, march 2015.
- [20] Baktash A, Vahedi A, Masoum M. *Improved switching table for Direct Power Control of three-phase PWM rectifier*. Proceedings of Australasian Universities Power Engineering Conference, AUPEC; 2007 :1-5.
- [21] Rodriguez P, Luna A, Ciobotaru M, Teodorescu R, Blaabjerg F. *Advanced Grid Synchronization System for Power Converters under Unbalanced and Distorted Operating Conditions*. in Proc. IEEE Ind. Electron. Conf. (IECON'06). 2006 : 5173-5178.
- [22] Rodriguez P, Luna A, Etxeberria I, Hermoso, J R, Teodorescu R . *Multiple second order generalized integrators for harmonic synchronization of power converters*. Energy Conversion Congress and Exposition, 2009. ECCE 2009. IEEE , 20-24 Sept. 2009 : 2239-2246
- [23] Hu J, Zhu J, Dorrell D G. New Control Method of Cascaded Brushless Doubly Fed Induction Generators Using Direct Power Control. *IEEE Transactions On Energy Conversion*. 2014 ; 29(3) : 771 - 779.
- [24] Bouafia A, Gaubert J.P, Chaoui A. Direct Power Control Scheme Based on Disturbance Rejection Principle for Three-Phase PWM AC/DC Converter under Different Input Voltage Conditions. *J. Electrical Systems*. 2012 ; 8(4) :367-383.

A. Rahab "Direct Power Control of Three Phase PWM Rectifier based DSOGI-VF Estimator for No-Ideal Line Voltages Conditions." *International Journal of Engineering Research and Applications (IJERA)* , vol. 8, no. 1, 2017, pp. 10-18.